

Phase-only modulation of a twisted nematic liquid-crystal TV by use of the eigenpolarization states

J. L. Pezzaniti and R. A. Chipman

University of Alabama in Huntsville, Optics Building 318, Huntsville, Alabama 35899

Received May 10, 1993

We present the eigenpolarization states of a commercially available liquid-crystal television display and show that phase-only modulation can be achieved over a large dynamic range of video voltages for several bias voltage settings if the eigenpolarization states are used. A set of operating curves using these polarization states is given for the device.

The phase-modulating properties of twisted nematic liquid-crystal spatial light modulators and liquid-crystal television (LCTV) displays have been investigated by several authors.¹⁻⁵ These investigations have concentrated primarily on achieving phase modulation in twisted nematic liquid-crystal devices while minimizing the polarization state modulation inherent in the twisted nematic cell. Konforti *et al.*² demonstrated that one could use liquid crystals as phase-only modulators by setting the bias voltage applied to the liquid crystal below the optical threshold, the voltage level at which disruption occurs of the spiral twist, and illuminating the liquid crystal with light linearly polarized parallel to the liquid crystal's molecular director. Other investigators^{3,6} have achieved phase-only modulation by double passing the light under modulation through the device so that the polarization change in the forward direction is compensated for by a reflection and traversing the device in the opposite direction. In this Letter we present the measured eigenpolarization states of an InFocus TVT-6000 LCTV for all gray levels between 0 and 255 and show that the eigenpolarization states remain nearly constant as functions of gray level for several bias voltage settings. We show that if the TVT-6000 LCTV is illuminated with an elliptical polarization state that is close to an eigenpolarization state of a LCTV pixel in any gray-level state, then phase-only modulation can be achieved in transmission without limiting the level of the applied bias voltage. As much as 195° of phase difference between off and on states (0 and 255 gray level) occurs when the LCTV is illuminated with an eigenpolarization state, with minimal associated polarization state modulation.

The eigenpolarization states of the LCTV were computed from the Mueller matrix measured for each gray level within the LCTV's dynamic range, for several brightness and contrast settings. Figure 1 shows the Mueller matrix of the LCTV as a function of video voltage. The brightness and contrast have been set to maximum, which we will see below provides the greatest amount of phase modulation. The Mueller matrix has two eigenvectors, which are physically realizable. These eigenvectors correspond to eigenpolarization states that are transmitted without change of polarization. The two eigenpolarization

states for the LCTV with maximum brightness and contrast levels are shown as functions of video voltage in Fig. 2. The average of these eigenpolarization states, given by

$$\mathbf{S} = \frac{1}{256} \sum_{n=0}^{255} \mathbf{S}_{\text{eigen},n} \quad (1)$$

where $\mathbf{S}_{\text{eigen},n}$ is the eigenpolarization state of the n th gray level, are used below to measure the operating curves for the device. The average eigenpolarization states for the LCTV with maximum brightness and contrast are

$$\mathbf{S}_r = \begin{pmatrix} 1.00 \\ 0.24 \\ -0.58 \\ 0.78 \end{pmatrix}, \quad \mathbf{S}_l = \begin{pmatrix} 1.00 \\ -0.24 \\ 0.58 \\ -0.78 \end{pmatrix}, \quad (2)$$

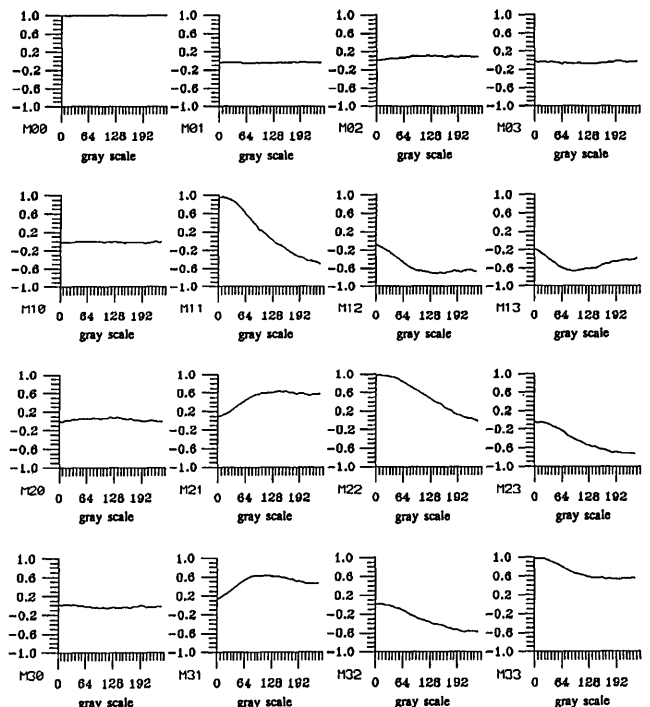


Fig. 1. Mueller matrix of the TVT-6000 LCTV as a function of video voltage. Brightness and contrast levels are set to maximum.

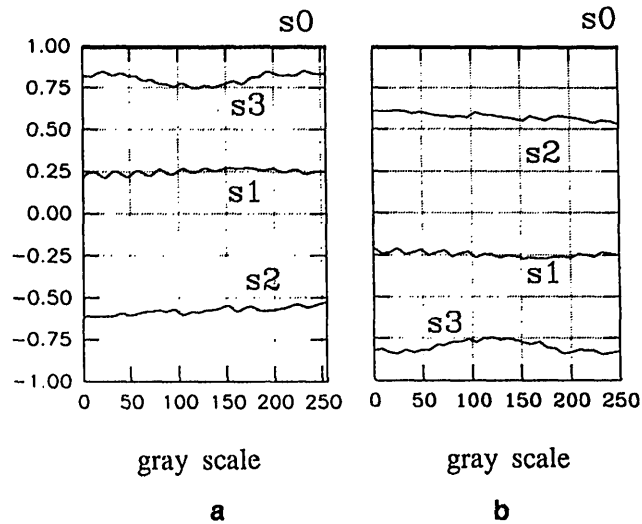


Fig. 2. Eigenpolarization states of the TVT-6000 LCTV as a function of video voltage: a, $S_{r,n}$; b, $S_{l,n}$.

where r and l indicate right and left helicity, respectively.

These measurements were repeated for various settings of the brightness and contrast controls. The averaged eigenpolarization states changed slightly with brightness and contrast settings (see Table 1).

Figure 3 is a schematic of the imaging polarimeter used to measure the Mueller matrices of the LCTV. The polarimeter had three sections: a polarization-state generator, a sample compartment, and a polarization-state analyzer. The polarization-state generator included a spatially filtered and coherence scrambled laser whose power was monitored by a reference detector. A collimated 20-mm-diameter beam passed through a stationary linear polarizer, followed by a $\lambda/3$ -wave linear retarder whose orientation was varied. The center 256×256 pixels of the LCTV were illuminated with the collimated beam at normal incidence. The LCTV was positioned such that the molecular director was aligned with the horizontal, and the electrodes addressing the beam emerged. The ribbon cable came out of the top of the device. The center portion of the 256×256 area of the LCTV was imaged onto 256×256 pixels of the imaging polarimeter's CCD. The gray scale addressing the LCTV pixels varied from 0 gray scale along the bottom row of pixels to 255 along the top row of LCTV. Data were collected on a central 256×16 subarray of the CCD such that the bottom row of CCD subarray collected light from the top row of LCTV pixels set at the 255 gray level. The subarray was averaged across the horizontal

rows of 16 pixels, leaving a vertical strip that corresponds to a one-to-one mapping between the linear gray-scale gradient on the LCTV to the subarray on the CCD. The beam leaving the device was analyzed by the polarization-state analyzer, another $\lambda/3$ wave retarder, and a stationary linear polarizer. A set of 60 plane waves with different polarization states was sequentially launched into the LCTV and analyzed by the polarization state analyzer. Sixty CCD images were digitized between rotations of the retarders, and a Mueller matrix was computed from the intensity values recorded at each CCD pixel. Extensive calibration procedures reduced systematic errors caused by nonideal polarization components and drift.^{7,8}

Intensity transmittance and phase shifts were measured with the four averaged eigenpolarization states for the set of four associated brightness and contrast settings summarized in Table 1. We measured the phase shifts for several video voltage levels by placing the device in one arm of a Mach-Zehnder interferometer, as illustrated in Fig. 4, and observing the movement of the interference fringes. For each test

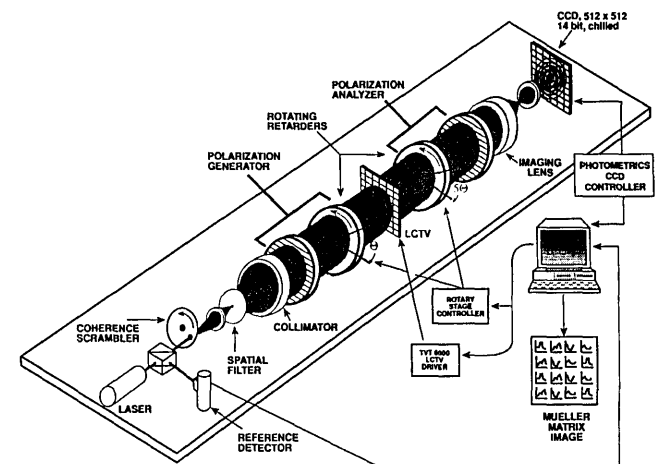


Fig. 3. Mueller matrix imaging polarimeter configured to measure the Mueller matrix of a LCTV.

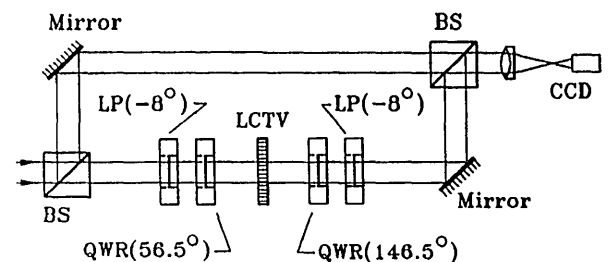


Fig. 4. Mach-Zehnder setup to measure the phase modulation of a LCTV. LP's, linear polarizers; QWR's, quarter-wave retarders; BS's, beam splitters.

Table 1. Averaged Eigenpolarization States of TVT-6000 for Various Brightness and Contrast Settings

	Maximum Brightness	Midrange Brightness
Maximum contrast	$S_r = (1.00, 0.24, -0.58, 0.78)^T$ $S_l = (1.00, -0.24, 0.58, -0.78)^T$	$S_r = (1.00, 0.23, -0.57, 0.79)^T$ $S_l = (1.00, -0.23, 0.57, -0.79)^T$
Midrange contrast	$S_r = (1.00, 0.24, -0.56, 0.79)^T$ $S_l = (1.00, -0.24, 0.56, -0.79)^T$	$S_r = (1.00, 0.24, -0.55, 0.80)^T$ $S_l = (1.00, -0.24, 0.55, -0.80)^T$

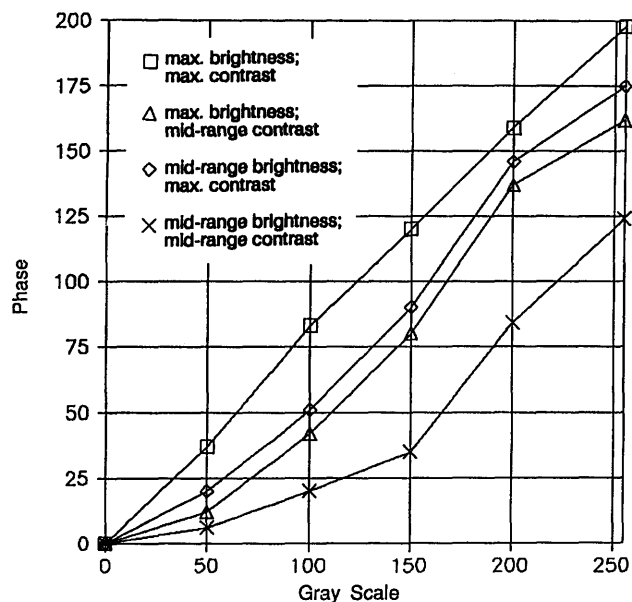


Fig. 5. Phase modulation as a function of video voltage for various brightness and contrast settings.

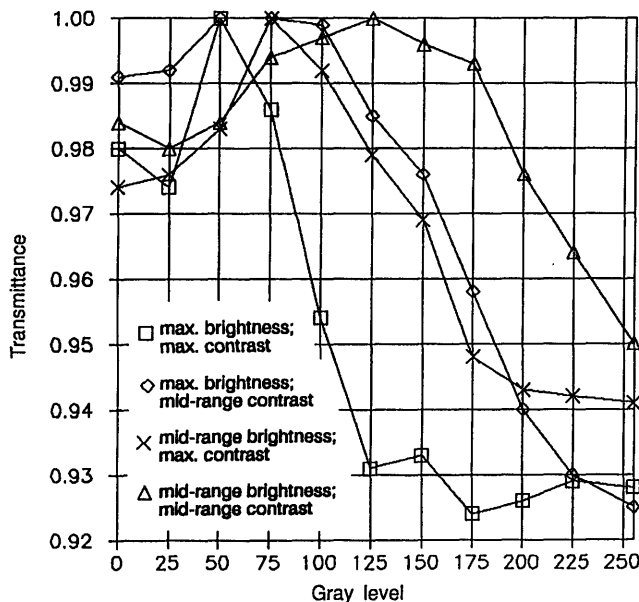


Fig. 6. Intensity transmittance as a function of video voltage for various brightness and contrast settings.

the polarization-state generator and the polarization-state analyzer were set to produce and accept the state S_i corresponding to the particular setting of brightness and contrast used for that test. The generator and analyzer settings shown in Fig. 4 are those used to produce and analyze the polarization

states associated with the maximum brightness and contrast levels. Only the state with left helicity, S_l , displayed a significant amount of phase modulation; the S_r state displayed $<0.1\pi$. The phase modulation of the S_l state for the four settings of brightness and contrast are plotted against the video gray level in Fig. 5. The greatest amount of phase modulation was found for maximum brightness and contrast settings.

To test the intensity transmittance through the polarization-state generator, LCTV, and polarization-state analyzer combination, we blocked the reference arm of the Mach-Zehnder interferometer and measured the transmittance in increments of 25 gray levels. The intensity transmittance curves could also be obtained with the Mueller matrix; this additional set of measurements provides a confirmation of the results obtained from the Mueller matrix. The transmittances have been normalized to the state of highest transmittance. Figure 6 shows the results. The variations in transmittance are due to slight changes in the eigenpolarization states. The smallest variation of transmittance was found when the brightness and contrast controls were set to midrange, halfway between the maximum and minimum settings. The largest variation, $\sim 7\%$, was found for the maximum settings of brightness and contrast.

In conclusion, the LCTV is an electrically addressable elliptical retarder, with elliptical eigenpolarization states. The retardance magnitude changes with applied voltage, but the retardance orientation, defined by its eigenpolarization states, remains nearly constant. The phase modulation of the polarization state with right helicity is small; nearly all phase modulation is associated with the polarization state with left helicity (the helicity of the liquid-crystal nematic spiral is unknown).

References

1. W. P. Belha, L. T. Lipton, E. Wiener-Avneer, J. Ginberg, P. G. Reif, D. Cassent, H. B. Brown, and B. V. Markevitch, *Opt. Eng.* **17**, 371 (1978).
2. N. Konforti, E. Marom, and S. T. Wu, *Opt. Lett.* **13**, 251 (1988).
3. T. H. Barnes, T. E. Eiji, K. Matusuda, and N. Ooyama, *Appl. Opt.* **28**, 4845 (1989).
4. D. A. Gregory, J. A. Loudin, J. C. Kirsch, E. C. Tam, and F. T. S. Yu, *Appl. Opt.* **30**, 1374 (1991).
5. K. Lu and B. E. A. Saleh, *Opt. Eng.* **29**, 240 (1990).
6. K. Lu and B. E. A. Saleh, *Appl. Opt.* **30**, 2354 (1991).
7. J. L. Pezzaniti and R. A. Chipman, *Proc. Soc. Photo-Opt. Instrum. Eng.* **1317**, 280 (1990).
8. D. B. Chenault, J. L. Pezzaniti, and R. A. Chipman, *Proc. Soc. Photo-Opt. Instrum. Eng.* **1746**, 231 (1992).